

# H $\alpha$ Imaging of Early-Type(Sa-Sab) Spiral Galaxies I<sup>1</sup>

Salman Hameed<sup>2</sup>, Nick Devereux<sup>2</sup>

Astronomy Department, New Mexico State University, Las Cruces, NM 88003

## ABSTRACT

H $\alpha$  and continuum images are presented for 27 nearby early-type(Sa-Sab) spiral galaxies. Contrary to popular perception, the images reveal copious massive star formation in some of these galaxies. A determination of the H $\alpha$  morphology and a measure of the H $\alpha$  luminosity suggests that early-type spirals can be classified into two broad categories based on the luminosity of largest H II region in the disk. The first category includes galaxies for which the individual H II regions have  $L_{H\alpha} < 10^{39} \text{ ergs}^{-1}$ . Most of the category 1 galaxies appear to be morphologically undisturbed, but show a wide diversity in nuclear H $\alpha$  properties. The second category includes galaxies which have at least one H II region in the disk with  $L_{H\alpha} \geq 10^{39} \text{ ergs}^{-1}$ . All category 2 galaxies show either prominent dust lanes or other morphological peculiarities such as tidal tails which suggests that the anomalously luminous H II regions in category 2 galaxies may have formed as a result of a recent interaction. The observations, which are part of an on-going H $\alpha$  survey, reveal early-type spirals to be a heterogeneous class of galaxies that are evolving in the current epoch.

We have also identified some systematic differences between the classifications of spiral galaxies in the Second General Catalog (RC2) and the Revised Shapley-Ames Catalog (RSA) which may be traced to subtle variations in the application of the criteria used for classifying spiral galaxies. An examination of earlier studies suggests that perceptions concerning the Hubble type dependence of star formation rates among spiral galaxies depends on the choice of catalog.

*Subject headings:* galaxies: interactions — galaxies: spiral — HII regions — stars: formation

---

<sup>1</sup>Based on observations obtained with the 1.5-meter telescope at CTIO and the 3.5-meter telescope at Apache Point Observatory (APO). The APO 3.5m telescope is owned and operated by the Astrophysical Research Consortium.

<sup>2</sup>Visiting Astronomer, Cerro Tololo Inter-American Observatory. CTIO is operated by the Association of Universities for Research in Astronomy, Inc. (AURA) under cooperative agreement with the National Science Foundation.

## 1. Introduction

An outstanding problem in extra-galactic astronomy is understanding the parameters that determine the structure and evolution of galaxies. A first step towards understanding the physical properties of galaxies is classification based on morphology.

Spiral galaxies were first classified by Hubble according to the size of the bulge, the tightness with which the spiral arms are wound, and the resolution of individual H II regions (Hubble 1936; de Vaucouleurs 1959). Several observational studies have elucidated differences among galaxies along the Hubble sequence (for a review see Roberts & Haynes 1994; Kennicutt 1998). Observations plus modeling of broad band colors of galaxies reveal that the bulge dominated Sa galaxies are red compared to the disk dominated Sc galaxies, suggesting an older population (Larson & Tinsley 1974). Similarly, Roberts(1969) measured the atomic gas content of 75 spiral galaxies and found that the ratio,  $M(\text{HI})/L(\text{B})$ , decreases systematically from the late-type spirals to the early-type Sa galaxies, suggesting early types to be deficient in hydrogen gas, compared to the late types.

The star formation history of galaxies can be traced using the integrated  $\text{H}\alpha$  equivalent widths, where the  $\text{H}\alpha$  emission line flux is normalized by the past star formation rate through the red continuum. Kennicutt & Kent (1983) measured the  $\text{H}\alpha$  equivalent widths for  $\sim 200$  spiral galaxies and demonstrated that the  $\text{H}\alpha$  equivalent widths decrease systematically from late-type spirals to early-type spiral galaxies, suggesting early-types to be deficient in massive young stars compared to the late types.

There are other observational results, however, which suggest that early-type spirals are not so quiescent. A recent Hubble Space Telescope(HST) study of the bulges of 75 spiral galaxies (Carollo *et al.* 1998) reveals a wide variety of activity, including star formation, hidden underneath the bulges of early-type spirals. Young & Knezek (1989) have showed that the dominant phase of the interstellar medium in Sa-Sab types is molecular, not atomic and that the molecular fraction is much higher in the early-types compared to the later types. The result, however, has been recently challenged by Casoli *et al.* (1998), who find that molecular gas comprises only about one third to one fourth of the total gas content of spirals of types Sa through Sc.

A recent analysis of the Infrared Astronomical Satellite (IRAS) database by Devereux & Hameed (1997) suggests that the global massive star formation rates, as determined by 60 micron luminosity functions, are comparable in early and late-type spirals. Similarly, far infrared to blue luminosity ratios of a large sample of nearby spiral galaxies do not show any morphological dependence (Tomita *et al.* 1996; Devereux & Hameed 1997). Evidently, the IRAS data has revealed a previously unsuspected population of early-type spirals with

high massive star formation rates.

The IRAS results, do not support previous claims, based on H $\alpha$  equivalent widths, that massive star formation rates increase along the Hubble sequence from Sa to Sc (Kennicutt 1983; Kennicutt *et al.* 1994). Part of the problem is that the sample of early-type spirals selected by Kennicutt (1983) and Kennicutt (1994) is small in number and is biased towards galaxies with low values of L(FIR)/L(B) (Devereux & Hameed 1997; Usui *et al.* 1998). We are, therefore, conducting an H $\alpha$  imaging survey of *all known* nearby early-type spiral galaxies in order to better understand the differences between the IRAS results and those of existing H $\alpha$  studies.

High resolution H $\alpha$  images of nearby galaxies provide important information about the morphology and luminosity of the ionized hydrogen gas. Surprisingly few H $\alpha$  images of early-type spirals exist in the published literature. The general notion that early-type spirals do not have significant massive star formation is, at least partially, responsible for the dearth of H $\alpha$  observations (Young *et al.* 1996). The continuum morphology of early-type spirals is dominated by an 'inert' stellar bulge which can hide star forming complexes that lie underneath them. CCD imaging allows the hidden H II regions to be revealed by subtracting the overwhelming continuum light.

Despite the dearth of H $\alpha$  images, our appreciation of the heterogeneous nature of early-type spirals has evolved considerably in the past quarter century. Van den Bergh (1976) and Kormendy (1977) found no H II regions in NGC 4594 and NGC 2841, leading them to speculate that the IMF in early-type spirals may be biased against the formation of massive stars. Later studies, however, showed that H II regions are indeed present in these particular galaxies (Schweizer 1978; Hodge & Kennicutt 1983; Kennicutt 1988). A detailed study of H II regions in the disks of seven Sa galaxies by Caldwell *et al.* (1991) found that H II regions are quite abundant in the disks but are significantly smaller than those in late-type spirals. Specifically, Caldwell *et al.* found that there are no H II regions in the disks of early-type spirals with luminosities  $> 10^{39} \text{ergs}^{-1}$ .

The purpose of the present paper is to report that H II regions are not only abundant in early-type spirals but some contain giant H II regions that are comparable in size and luminosity to giant H II regions seen in late-type spirals. Our findings support recent H $\alpha$  observations by Young *et al.* (1996) and Usui *et al.* (1998), who have also identified numerous early-type spirals with star formation rates comparable to the most prolifically star forming late-type spirals.

In order to quantify the diverse star forming capabilities of early-type spirals, we are conducting a systematic program of H $\alpha$  imaging. The results are presented here for twenty

seven galaxies imaged to date. The sample is described in section 2 and the observations are described in section 3. The results are presented in section 4, followed by discussion in section 5.

## 2. The Sample

An H $\alpha$  imaging survey is being conducted to investigate the star forming capabilities of nearby early-type (Sa-Sab) spiral galaxies. The target galaxies have been selected from the Nearby Galaxy Catalog (NBG)(Tully 1988) which is the largest complete compilation of bright galaxies with velocity less than  $3000\text{km/s}$ , corresponding to a distance of 40 Mpc ( $H_0 = 75\text{kms}^{-1}/\text{Mpc}$ ). The target galaxies are listed in Table 1 with some useful observables. Distances in the NBG catalog are based on a Virgo-centric in-fall model (Tully 1988). The NBG catalog also lists morphological types for each galaxy

The complete sample includes all (57) bright,  $m(B) \leq 12.1$  magnitude, non-interacting early-type (Sa-Sab) spirals known within 40 Mpc. For the purposes of the present work, “interacting” galaxies are defined as those which have cataloged companions within  $6'$  of each other.

The goal of the survey is to image the complete sample of nearby early-type spirals. Imaging the largest complete sample will circumvent incompleteness corrections and minimize statistical errors in quantifying the incidence of nuclear starbursts, nuclear emission line spirals, nuclear point sources, and other morphological peculiarities in nearby early-type spirals. So far we have imaged twenty-one galaxies, the results of which are presented in this paper.

As part of a complimentary study we are also obtaining H $\alpha$  images of twenty-one far-infrared luminous early-type spirals, identified by Devereux and Hameed (1997). Fifteen of these galaxies have  $m(B) \leq 12.1$  and, hence, are already included in the complete sample described above. The remaining six galaxies have been imaged and they are included in this paper also.

## 3. Observations

Observations of northern hemisphere galaxies were obtained with the Astrophysical Research Consortium (ARC) 3.5m telescope at Apache Point Observatory (APO) in New Mexico. Southern hemisphere galaxies were observed with the 1.5m telescope at Cerro Tololo Inter-American Observatory (CTIO) in Chile.

Six northern hemisphere early-type spiral galaxies were observed using the Double Imaging Spectrograph (DIS) at APO between August 1996 and January 1997. The Texas Instruments CCD chip has a pixel scale of  $0.61''\text{pixel}^{-1}$  and a  $4.2'$  field of view. Two red-shifted narrow band  $\text{H}\alpha + [\text{NII}]$  ( $6570\text{\AA} \& 6610\text{\AA}$ ,  $\Delta\lambda = 72\text{\AA}$ ) filters and a line free red continuum ( $6450\text{\AA}$ ,  $\Delta\lambda = 120\text{\AA}$ ) filter were used to obtain the line and continuum images, respectively. Three exposures were obtained through each of the line and continuum filters. Details of the observations are summarized in Table 2.

Twenty-one southern hemisphere galaxies were observed using the Cassegrain Focus CCD Imager (CFCCD) on the CTIO 1.5m telescope. CFCCD uses a  $2048 \times 2048$  Tektronics chip and has a pixel scale of  $0.43''\text{pixel}^{-1}$  at  $f/7.5$ , yielding a field of view of  $14.7' \times 14.7'$ . All of the galaxies were imaged using the narrow band  $\text{H}\alpha + [\text{NII}]$  filter at  $6606\text{\AA}$  ( $\Delta\lambda = 75\text{\AA}$ ) with the exception of NGC 5728 for which we used the  $\text{H}\alpha + [\text{NII}]$  filter at  $6649\text{\AA}$  ( $\Delta\lambda = 76\text{\AA}$ ). The narrow band line free red continuum filter for all the galaxies was centered at  $6477\text{\AA}$  ( $\Delta\lambda = 75\text{\AA}$ ). Three exposures of 900 seconds were obtained through each of the line and the continuum filters for all the southern hemisphere galaxies (see Table 2).

### 3.1. Data Reduction

The Image Reduction Analysis Facility (IRAF) software package was used to process the images. The images were bias subtracted, and then flat fielded using twilight flats taken on the same night as the galaxy data. Sky subtraction was achieved by measuring the sky level around the galaxy and then subtracting it from the images. Images were then registered and median combined to improve the S/N ratio and eliminate cosmic rays.

The continuum image was then scaled to the line plus continuum image by measuring the integrated fluxes of several ( $\geq 10$ ) stars common to both images. The final  $\text{H}\alpha$  image was obtained by subtracting the scaled continuum image from the  $\text{H}\alpha + \text{continuum}$  image to remove foreground stars and the galaxy continuum.

The  $\text{H}\alpha$  images were flux calibrated using observations of the standard stars G1912B2B and BD +28°4211 (Massey *et al.* 1988) for the northern hemisphere galaxies and LTT 3218, LTT 1020, and LTT 7987 (Hamuy *et al.* 1994) for the southern hemisphere galaxies (see Table 2). The observing conditions were photometric, with  $< 10\%$  variations in the standard star fluxes, for all of the imaging observations.

There are several factors that contribute to the uncertainties in the determination of  $\text{H}\alpha$  flux measurements. Large systematic errors may be introduced by the continuum subtraction procedure. Small random errors are introduced by read noise in the detector

and photon noise but these are negligible compared to the uncertainty introduced by the continuum subtraction procedure.

There are two factors that contribute to the uncertainty in determining the continuum level. First, one assumes that the foreground stars used for estimating continuum level have the same intrinsic color as the galaxy. Second, one must assume that the galaxy has the same color everywhere. Both assumptions are unlikely to be correct. Unfortunately the uncertainty in the  $H\alpha$  flux depends sensitively and non-linearly on the continuum level subtracted. It has been determined empirically that 2% – 4% errors in the continuum level correspond to 10% – 50% errors in the  $H\alpha$  flux, depending on the relative contribution of the continuum light.

The  $H\alpha$  fluxes are presented in Table 3 along with the calculated  $H\alpha$  luminosities. The  $H\alpha$  fluxes include contributions from the satellite [NII] lines at  $\lambda\lambda$  6548,6584 and have not been corrected for Galactic or internal extinction. Kennicutt and Kent (1983) suggest that the average extinction in their sample is typically  $\sim 1$  mag. The  $H\alpha$  extinction, however, is expected to be more for galaxies that have high inclinations or those that harbor nuclear starbursts. We have not applied extinction corrections due to the uncertainties involved in determining its true value. Consequently the  $H\alpha$  fluxes and luminosities presented in Table 3 are lower limits to the intrinsic  $H\alpha$  fluxes and luminosities.

### 3.2. Comparison with Previous Measurements

Seven of the galaxies presented in this paper already have published  $H\alpha$  fluxes. Figure 1 compares our measured values in the same apertures as those in the literature. The agreement between the measurements is, in general, good. NGC 1433 and NGC 7552, in particular, provide a good test as both ours and the comparison observations (Crocker *et al.* 1996 and Lehnert & Heckman 1995 respectively) were made with the 1.5m telescope at CTIO and the measurements are in good ( $< 11\%$ ) agreement with each other.

The biggest discrepancy is with NGC 1022, where our  $H\alpha$  flux is 68% higher than the value published by Kennicutt & Kent (1983). However, our measured flux for NGC 1022 is within 8% of the value obtained by Usui *et al.* (1998).

## 4. Results

#### 4.1. Classification of Early-type Spirals

A study of the H II region luminosity functions in the disks of seven Sa galaxies by Caldwell *et al.*(1991) showed that while H II regions are abundant, there are none with H $\alpha$  luminosities  $> 10^{39} \text{ergs}^{-1}$ . Our results confirm that the H $\alpha$  luminosity of H II regions in most early-type spirals is less than  $10^{39} \text{ergs}^{-1}$ . However, we also find that a significant fraction (15 – 20%) of early-type spirals do have at least one H II region in the disk with  $L_{H\alpha} \geq 10^{39} \text{ergs}^{-1}$ . The latter result is not necessarily in contrast to Caldwell’s study for two reasons. First, Caldwell *et al.* had a small sample containing only seven galaxies and could have easily missed early-type spirals with giant H II regions. Second, their sample contained only Sa galaxies, whereas early-type spirals discussed in this paper include both Sa and Sab types.

Early-type spirals have been divided in two categories based on the H $\alpha$  luminosity of the largest H II region present in the disk. The H $\alpha$  luminosity of the individual H II regions in the disks of all category 1 galaxies is less than  $10^{39} \text{ergs}^{-1}$ , whereas category 2 galaxies contain at least one H II region in the disk with  $L_{H\alpha} \geq 10^{39} \text{ergs}^{-1}$ .

Figure 2 shows the range of global H $\alpha$  luminosities for the two categories of Sa-Sab galaxies. Perhaps not surprisingly, category 2 galaxies dominate at high,  $L_{H\alpha} > 1.7 \times 10^{41} \text{ergs}^{-1}$ , luminosities. A two-tailed Kolmogorov-Smirnov(KS) test indicates that the two categories of galaxies are not derived from the same population at a confidence level greater than 99%. Similarly, Figure 3 shows the range of H $\alpha$  equivalent widths, where the continuum-free line flux is normalized by the red continuum, for the two categories of early-type spirals. The K-S test again reveals that the two categories of galaxies are not derived from the same population at a confidence level greater than 99%.

In order to verify that the difference in the distribution of global H $\alpha$  luminosities between the two categories is not related to the nuclear properties, the histograms of nuclear(1 kpc) H $\alpha$  luminosities are compared in Figure 4. The K-S test reveals that the difference between the distributions in Figure 4 is insufficient to reject the null hypothesis that the two categories are drawn from the same population. Thus the difference between the two categories of early-type spirals is primarily a global phenomenon unrelated to their nuclei.

In addition to the statistical tests described above, we varied the H $\alpha$  luminosity of the largest H II region in each galaxy by 20% to further verify the dichotomy in the properties of category 1 and 2 early-type spirals. Indeed, a 20 percent variation, which represents a typical uncertainty in H $\alpha$  measurements of individual H II regions, has no effect on the distribution of galaxies between the two categories. We do want to stress, however, that

the purpose of this paper is to introduce early-type spirals with giant H II regions and to show that Sa-Sab galaxies are heterogeneous in nature. The sub-classification of early-type spirals into two categories has been done solely to investigate the conditions that may lead to the formation of luminous H II regions.

The continuum and continuum-subtracted H $\alpha$  images are shown in Figures 5, 6, & 7 and the observed properties of Sa-Sab galaxies are described in more detail below.

### *Category 1 Early-type Spirals*

H II regions in category 1 galaxies are either small or totally absent from the spiral arms (see Figure 5). By definition, all H II regions in the disk of category 1 spirals have  $L_{H\alpha} < 10^{39} \text{ergs}^{-1}$ . Consistent with earlier studies (Kennicutt 1988; Caldwell *et al.* 1991; Bresolin & Kennicutt 1997), we find that H II regions in most early-type spirals contain only a few massive stars, whereas H II regions in late-type spirals can contain hundreds or even thousands of stars.

The seventeen galaxies included in category 1 resemble what most astronomers identify as classical early-type spirals. Morphologically, most category 1 galaxies appear undisturbed in the continuum image, but the H $\alpha$  images reveal very diverse nuclear properties.

*Extended nuclear emission line region (ENER):* There are seven category 1 galaxies (NGC 1350, NGC 1371, NGC 1398, NGC 1433, NGC 1515, NGC 1617, NGC 3169) in which an extended nuclear emission line region(ENER) has been detected. The detailed morphology of the ENER gas is difficult to discern at the distances of these galaxies, but they appear to be similar to the nuclear emission line spirals discovered in the centers of M81 (Jacoby *et al.* 1989; Devereux *et al.* 1995) and M31 (Jacoby *et al.* 1985; Devereux *et al.* 1996). It is clear that the filamentary emission line gas is quite different from the clumpy H II regions in the spiral arms. The ENER is most likely shock-ionized or photo-ionized by UV radiation from bulge post asymptotic giant branch stars (Devereux *et al.* 1995; Heckman 1996). All category 1 galaxies hosting extended nuclear emission line regions have the lowest nuclear H $\alpha$  luminosities.

*Nuclear Point Sources:* Of the remaining category 1 galaxies, five (NGC 2273, NGC 5188, NGC 5728, NGC 7172, NGC 7213) have an unresolved H $\alpha$  source at the nucleus. Apart from 5188, all four galaxies have been spectroscopically identified as Seyferts(NGC 2273: Ho *et al.* 1997a; NGC 5728: Phillips *et al.* 1983; NGC 7172: Sharples *et al.* 1984; NGC 7213: Filippenko & Halpern 1984). NGC 2273, NGC 5728 and NGC 7172 have faint H II regions in their disk, whereas NGC 7213 has a number of H II regions in the circumnuclear region, but the disk is almost devoid of any H II regions. NGC 7213 also has



an extended nuclear emission line region surrounding the point source. NGC 5188 has prominent H II regions and its nucleus has been spectroscopically classified as an H II region by Veron-Cetty & Veron (1986).

*Nuclear starbursts:* The nuclei in four of the remaining category 1 galaxies (NGC 3471, NGC 1482, NGC 3885, NGC 1022) are resolved and contribute more than 50% of the total H $\alpha$  luminosity. NGC 1022 (Ashby *et al.* 1995), NGC 3471 (Balzano 1983) and NGC 3885 (Lehnert & Heckman 1995) have been spectroscopically identified as nuclear starbursts. No spectral confirmation is available in the literature for NGC 1482 but it has been included as a nuclear starburst galaxy based on similarities in morphology and H $\alpha$  luminosity to NGC 1022, NGC 3471, and NGC 3885. It is worthwhile to mention that all four galaxies also have very high far infrared luminosities,  $\geq 10^{10} L_{\odot}$  (Devereux & Hameed 1997), comparable to the prototypical starburst galaxy M82 (Rieke *et al.* 1980). Dust lanes are prominent in all four galaxies and there are virtually no H II regions in their disks.

NGC 3717 has a high inclination and could not be classified into any of the above sub-groups. Spectroscopically, the nucleus of NGC 3717 has been classified as an H II region by Veron-Cetty & Veron (1986).

### *Category 2 Early-type Spirals*

Eight of the galaxies presented in this paper have at least one disk H II region with  $L_{H\alpha} \geq 10^{39} \text{ergs}^{-1}$  defining a new category of early-type spirals (see Figure 6).

Dust lanes or tidal tails are present in all category 2 galaxies. Despite the fact that extinction is an important factor in these dusty galaxies, early-type spirals with the highest H $\alpha$  luminosity belong exclusively to category 2 (Figure 2). Additionally, all category 2 galaxies have far-infrared luminosities in excess of  $10^{10} L_{\odot}$  (Devereux & Hameed 1997).

The discovery of a significant number of early-type spirals with H $\alpha$  luminosities comparable to those produced by the most prolifically star forming late-type spirals is surprising, as early-type spirals are widely believed to have massive star formation rates that are considerably lower. Based on the available images and far-infrared luminosities of the entire sample, it is estimated that category 2 galaxies could represent 15% – 20% of all early-type spirals in the nearby ( $D \leq 40 \text{Mpc}$ ) universe, a significant group that can no longer be ignored as oddities.

The continuum images of two category 2 galaxies (NGC 986, NGC 7552) reveal the possible existence of previously uncataloged dwarf galaxies that appear to be interacting with the larger galaxies. Redshift information is not yet available for either of the dwarf

galaxies so the physical association cannot be confirmed. Nevertheless, if the dwarf galaxy seen at the end of the northern spiral arm in NGC 7552 is indeed associated with NGC 7552, it has an absolute magnitude of -12.95 in R which is comparable to some of the dwarf galaxies seen around M31 and the Milky Way. There is no detectable H $\alpha$  emission from the dwarf companion of NGC 7552.

In the case of NGC 986, the dwarf galaxy is located at the end of the north-eastern spiral arm and appears to be in the process of being tidally disrupted. The distorted shape of the dwarf along with the contribution of stars in the spiral arms of NGC 986 makes it difficult to measure its magnitude with any certainty. Nevertheless, the presence of interacting dwarfs exclusively in category 2 galaxies may be related to the existence of giant H II regions in these galaxies.

Two category 2 galaxies (NGC 7582, NGC 6810) have been optically classified as Seyferts. The presence of Seyferts in both categories of early-type spirals suggest that the incidence of Seyfert activity is unrelated to the phenomenon that is responsible for the global differences between category 1 and category 2 galaxies.

### *Unclassified*

Surprisingly, NGC 660 and NGC 2146 apparently have no disk H II regions with  $L_{H\alpha} \geq 10^{39} \text{ ergs}^{-1}$  but both have high far infrared luminosity (Devereux & Hameed 1997) and a morphology that appears to be even more disturbed than any of the category 2 galaxies (see Figure 7). The apparent absence of luminous H II regions may be a consequence of the 13 and 9 magnitudes of extinction in the V band for NGC 660 and NGC 2146 respectively (Young *et al.* 1988). Nevertheless, we have not classified these two galaxies as they cannot be unambiguously placed into either category.

## **4.2. H II Region Luminosity Functions**

In order to understand some of the properties of H II regions in the two categories of early-type spirals, we derived H $\alpha$  luminosity functions for the H II regions in a category 1 galaxy, NGC 1398, and a category 2 galaxy, NGC 7552. The two galaxies were chosen because they are at a comparable distance (16.1 Mpc & 19.5 Mpc for NGC 1398 & NGC 7552 respectively), they have relatively low inclinations, and they provide a good contrast between the two categories of early-type spirals.

*Measurement of H II region H $\alpha$  fluxes*

Individual H II regions in the two galaxies were identified computationally using the DAOfind routine incorporated in an IDL program, 'HIIphot', developed by Thilker *et al.* 1999. The program identifies local maxima by using Gaussian kernels comparable, and slightly larger than the effective resolution, on the original image and also on several smoothed versions.

Earlier studies of luminosity functions have mostly assumed a symmetrical shape for the H II regions.(e.g. Kennicutt *et al.* 1989; Caldwell *et al.* 1991). In nature, however, H II regions are observed to be asymmetrical. The attribute of HIIphot is that it provides the freedom for H II regions to acquire any shape. The H $\alpha$  flux was measured by summing the pixel values within each region. The local background level for each region was determined by the mode of the 'region-hugging' annulus having a specified physical width. The details of the 'HIIphot' program will be published elsewhere (Thilker *et al.* 1999).

### *Luminosity Functions*

The observed H $\alpha$  fluxes were converted into H $\alpha$  luminosities using the distances for NGC 1398 and NGC 7552 listed in Table 1. The striking difference between the H $\alpha$  images of NGC 1398 and NGC 7552 (see Figures 5 and 6 respectively) is also reflected in the widely dissimilar H II region luminosity functions as illustrated in Figure 8. In both cases, the *bright* H II regions have a luminosity function that is well represented by a power-law:

$$N(L) \propto L^\alpha dL$$

with exponent values of  $-2.4(\pm 0.2)$  and  $-2.0(\pm 0.1)$  for NGC 1398 and NGC 7552 respectively. Our slope for NGC 1398 is in good agreement with the slope obtained by Caldwell *et al.* for the same galaxy, whereas our value is steeper for NGC 7552 than the  $-1.7$  slope determined by Feinstein (1997).

The two categories of early-type spirals, as defined in this paper, are based on the H $\alpha$  luminosity of the largest H II region in the disk. The H II region luminosity functions show that H II regions, in general, are more luminous in the category 2 galaxy, NGC 7552, as compared to the category 1 galaxy, NGC 1398. We also, cautiously, report the difference in the shape of the two luminosity functions. NGC 1398 has a steep power law distribution. The H II region luminosity function for NGC 7552, on the other hand, is a Gaussian with a turnover luminosity located at least a factor of six higher than in NGC 1398. The two galaxies are at about the same distance and were observed on the same night with the 1.5m telescope at CTIO for the same integration time. Similarly the data was reduced in an identical manner and H II region luminosity functions were determined with 'HIIphot' using the same parameters for the two galaxies. So there is little doubt that the the difference in the shapes of the two luminosity functions is real and confirms the visual impression given

by H $\alpha$  images of NGC 1398 and NGC 7552 in Figures 5 and 6 respectively.

Thus the difference in global H $\alpha$  luminosities between the two categories of early-type spirals is not attributable to just one anomalous H II region, but rather suggests intrinsic differences in the ensemble of H II regions found in the two categories of early-type spirals. A subsequent paper will present a more detailed analysis of the H II region luminosity functions for nearby early-type spirals.

## 5. Discussion

Early-type spirals have, in the past, been associated with low massive star formation rates. The results presented in this paper, however, indicate that early-type spirals are a heterogeneous group of galaxies with a significant number of them showing star forming regions that are comparable in luminosity to those found in late-type spirals. Early-type spirals have been divided into two categories based on the H $\alpha$  luminosity of their largest H II region in the disk. H II regions in all category 1 galaxies have  $L_{H\alpha} < 10^{39} \text{ergs}^{-1}$ , whereas category 2 early-type spirals have at least one H II region with  $L_{H\alpha} \geq 10^{39} \text{ergs}^{-1}$ . The purpose of the following discussion is to elaborate on the diversity of early-type spirals as revealed by the H $\alpha$  and the continuum images.

### 5.1. Nuclear Diversity in Category 1 Galaxies

Most of the category 1 early-type spirals appear to be morphologically undisturbed. Despite the similarities in the continuum image, they have very diverse nuclear H $\alpha$  properties ranging from nuclear starbursts to low luminosity extended nuclear emission line regions (ENERs) to unresolved point sources. A recent, comprehensive, spectroscopic survey of the nuclei of nearby galaxies by Ho *et al.* (1997) revealed a similarly wide variety of spectroscopic phenomena including H II nuclei in 22%, LINERs in 36%, and Seyfert nuclei in 18% of early-type spirals. In addition, they have found that LINERs and Seyferts reside most frequently in early-type spiral galaxies. Unfortunately, we are presently unable to correlate all of the images presented in this paper with Ho's spectroscopic survey as most of our images are for the southern hemisphere whereas Ho's survey is for the northern hemisphere. However, we do have spectroscopic classifications for the nuclei of 17 galaxies that can be used to determine the correspondence between spectroscopy and morphology (Table 4).

All category 1 galaxies with unresolved H $\alpha$  nuclear point sources have been optically

classified as Seyferts except NGC 5188, which is classified as “H” by Veron Cetty & Veron (1986). Spectroscopic information is available for only 4 ENER category 1 early-type spirals but all 4 have a LINER or a Seyfert-like spectrum, classified as “N” by Veron-Cetty & Veron (1986). The spectra of Seyfert-like, “N”, galaxies have faint  $H\alpha$  and [NII] lines,  $H\alpha < 1.2 \times [NII]\lambda 6583$ , and no other detectable emission lines. The poor S/N of the data, make it impossible to distinguish between a Seyfert 2 and a LINER (Veron-Cetty & Veron 1986), however, we suspect that all ENER category 1 galaxies with “N” classification are LINERs. Conversely, we also suspect that not all LINERs are AGNs, as advocated recently by Ho *et al.* (1997).

The re-discovery of a possible correspondence between LINERs and extended emission line gas in the nuclei of spiral galaxies is not surprising. Keel (1983a), in an  $H\alpha$  imaging survey of the nuclei of spiral galaxies hosting LINER spectra, found extended emission in most cases. In addition, he found that LINER type spectra are ubiquitous in the nuclei of spiral galaxies not containing an H II region of much higher emission luminosity, which would make the low ionization region undetectable if present (Keel 1983b). Similarly, we have been able to detect ENERs only in galaxies with few or no H II regions in the nuclear region.

M31, the nearest spiral galaxy, hosts an extended nuclear emission line region (Rubin & Ford 1971; Jacoby *et al.* 1985) and provides an excellent opportunity to study the circumnuclear region in detail. The ENER in M31 spans 2 kpc (Devereux *et al.* 1994) and has a complex filamentary structure that is similar to the ENERs observed in more distant category 1 early-type spirals. The spectroscopic analysis of the ENER in M31 shows that it is indeed a LINER (Heckman 1996). The absence of a UV nuclear point source rules out an AGN as a source for photoionization of the emission line gas in M31. Similarly, HST observations have shown that the nuclear spiral in M31 is not ionized by massive stars (King *et al.* 1992; Devereux *et al.* 1994). Post-asymptotic giant branch (PAGB) stars provide a possible source of ionization for the gas in the nuclear region (Devereux *et al.* 1995; Heckman 1996) and Binette *et al.* (1994) have shown that photoionization by PAGB stars can lead to a LINER spectrum. Thus a LINER spectrum does not necessarily betray an AGN as advocated recently by Ho *et al.* (1996).

M81 is the nearest category 1 Sa-Sab spiral and it hosts a low luminosity LINER/Seyfert 1 nucleus (Filippenko & Sargent 1988; Ho *et al.* 1996). The presence of a broad line region (Peimbert & Torres-Peimbert 1981), a compact X-ray (Fabbiano 1988; Petre *et al.* 1993) and radio source (Beitenholz *et al.*), and a UV nuclear source (Devereux *et al.* 1997) strongly argue for the presence of a low luminosity AGN (Ho *et al.* 1996; Maoz *et al.* 1995). High resolution  $H\alpha$  imaging has also revealed an extended nuclear emission line spiral which

is strikingly similar to the one observed in M31 (Jacoby *et al.* 1989; Devereux *et al.* 1995). The spiral is not ionized by the spectroscopically identified AGN, as the Seyfert contributes < 5% of the total H $\alpha$  luminosity of the spiral (Devereux *et al.* 1995; Devereux *et al.* 1997). Furthermore, the extended emission line gas, like M31, has a LINER spectrum (Heckman, private communication). Recent HST observations have shown that the nuclear spiral in M81 is not ionized by massive stars (Devereux *et al.* 1995, 1997). The source of ionization for the nuclear spiral is unknown, but it is most likely shock-ionized or photo-ionized by UV radiation from bulge post asymptotic giant branch stars (Devereux *et al.* 1995). M81 is likely to be a composite object; a truly compact AGN surrounded by an extended emission line region like the one in M31.

The two nearest LINERS, M31 and M81, illustrate the need for both spectroscopic and imaging observations in order to distinguish between true AGNs and ENERs with spectra that look like AGN. The spectroscopic survey conducted by Ho *et al.* (1997a) included most of our northern hemisphere early-type spirals, which we are in the process of imaging. The new images will allow us to determine the extent to which the spectroscopically identified AGNs are responsible for ionizing the extended emission line gas seen under the bulges of early-type spirals.

## 5.2. Morphological Peculiarities in Category 2 Galaxies

In recent years it has been suggested that interactions may play an important role in the formation and subsequent evolution of early-type spirals (e.g. Schwiezer 1990, Pfenniger 1991, Zaritsky 1995). Furthermore, there is growing observational evidence to suggest that early-type spirals are perhaps the most dynamic of all the nearby galaxy systems. A recent HST survey of the bulges of nearby spiral galaxies has revealed that a significant fraction ( $\sim 40\%$ ) of early-type spirals show little or no morphological evidence for a smooth,  $R^{1/4}$  law (Carollo *et al.* 1998). Indeed, Schwiezer & Seitzer (1988) discovered ripples around some early-type spirals indicating that a major accretion event occurred in the past 1-2 Gyr. Similarly, the discovery of counter-rotating gas and star disks in the early-type spirals NGC 4826 (Braun *et al.* 1992) and NGC 7217 (Merrifield & Kuijken 1994) provide additional evidence for past interactions.

Perhaps galaxies classified as category 2 are the early-type spirals interacting in the current epoch. Note that we had excluded all galaxies that had cataloged companions within 6' and yet we still see signs of morphological disturbance in most of the category 2 galaxies. The discovery of previously unknown inter-lopings dwarf galaxies in two of the category 2 early-type spirals provides direct observational evidence for on-going interactions.

Other morphological peculiarities, such as tidal tails and dust lanes, are present in all category 2 galaxies providing further indirect evidence for interactions. Numerous H $\alpha$  and far-infrared studies indicate that interactions elevate massive star formation rates (e.g. Bushouse 1987, Kennicutt *et al.* 1987, Liu & Kennicutt 1995, Young *et al.* 1996). All of the category 2 galaxies have far-infrared luminosities in excess of  $10^{10}L_{\odot}$ , and populate the high end of the local H $\alpha$  luminosity function, both measures indicative of high rates of massive star formation that is clearly seen in H $\alpha$  images in the form of giant H II regions. It is interesting to note that the distinction between the two categories of early-type spirals is based only on the luminosity of the largest H II region in the disk, and yet this simple segregation leads to other clear differences in the range of global H $\alpha$  luminosities, galaxy morphology, and the range of individual H II region luminosities.

The presence of morphological peculiarities in a significant fraction of early-type spirals may be linked to the idea of forming big bulges through minor mergers. According to the numerical simulations of Mihos & Hernquist (1994), the merger of a dwarf galaxy with a disk galaxy can lead to the formation of a stellar bulge. A series of such mergers or accretion events could form the large bulges found in early-type spirals (Pfenninger 1993; Mihos & Hernquist 1994; Rich & Terndrup 1997).

Classical models of galaxy formation (Eggen *et al* 1962) predict bulges of galaxies to be old and metal rich. While the Galactic Bulge provides support for this theory, it may not be representative of all bulges. Recent observations of bulges have revealed them to be diverse and heterogeneous in nature (for a review see Wyse *et al.* 1997). Work on color gradients by Balcells & Palatier (1994) show that there is little or no color change between the disk and bulge for some early-type spirals. Bulge populations seem to resemble their parent disks, suggesting that bulges may not be significantly older. Similarly, blue bulges observed in several S0 galaxies (Schweizer 1990) (NGC 5102, NGC 3156, IC 2035 etc.) lend further support to the idea of bulge formation through minor mergers. Further work on stellar populations is needed to understand and quantify the diverse properties exhibited by the bulges in nearby early-type spiral galaxies.

### 5.3. *Influence of Bars on Early-type Spirals*

Several studies have been conducted to determine the influence of bars on star formation rates (e.g. Hawarden *et al.* 1986; Devereux 1987; Puxley *et al* 1988; Arsenault 1989; Ryder & Dopita 1994; Huang *et al.* 1996; Tomita *et al.* 1996; Ho *et al* 1997b ). Whereas, H $\alpha$  and far-infrared studies of large galaxy samples (Ryder & Dopita 1994; Tomita *et al.* 1996 respectively) find no correlation of global star formation with the presence of

bars, numerical models suggest that stellar bars can strongly perturb gas flows in disk, and trigger nuclear star formation. Indeed, nuclear star formation rates are measured to be preferentially higher for galaxies that have bars, especially in early-type spirals. Devereux (1987) measured strong nuclear  $10\mu\text{m}$  emission in 40% of barred early-type spirals, indicating high star formation rates. A similar excess was not observed in late-type barred spirals. To provide some measure of comparison the *nuclear* star formation rates in some barred early-type spirals are comparable to the globally integrated star formation rates of late-type spirals.

Enhanced nuclear star formation in early-type spirals may be related to the location of the inner Lindblad resonance (ILR) (Devereux 1987) which is dependent on the central mass distribution. The ILR in bulge-dominated Sa-Sab galaxies is expected to be located well inside the bar and close to the nucleus (Elmegreen & Elmegreen 1985), allowing a stellar bar to transfer gas from the disk region into the nuclear region more efficiently, prompting a nuclear starburst. However, the presence of a bar in an early-type spiral does not necessarily mean enhanced nuclear star formation. NGC 1398 and NGC 1433 (Figure 5) have prominent bars and yet they have little or no massive star formation in the nuclear region. Similarly, bars are not essential for the presence of a nuclear starburst as is illustrated by the starburst in the nucleus of non-barred galaxy, NGC 3885.

$\text{H}\alpha$  observations of a large sample of early-type spirals provide an excellent opportunity to study the effects of bars on these bulge-dominated Sa-Sab galaxies. Unfortunately, with our current data, we don't yet have enough statistics to analyze the influence of bars with any certainty. In our sample of 27 galaxies presented here, 17 have bars (including intermediate cases), 5 don't have bars, and no information is available for the remaining 5 galaxies (see Table 4). We will discuss early-type spirals in the context of bars in a later paper when we have obtained  $\text{H}\alpha$  images for the complete sample of nearby early-type spirals.

#### 5.4. *Star Formation in Early-type Spirals*

The star forming properties of galaxies can also be quantified using  $\text{H}\alpha$  equivalent widths, where the  $\text{H}\alpha$  flux is normalized by the red light representing the older stellar population. In essence, the  $\text{H}\alpha$  equivalent width measures the ratio of current star formation to past star formation. Figure 9 compares  $\text{H}\alpha$  equivalent widths for the galaxies presented in this paper with the early-type spirals observed by Kennicutt & Kent (1983) and Usui *et al.* (1998). Contrary to popular perception,  $\text{H}\alpha$  equivalent widths of early-type spirals presented in this paper reveal a significant fraction of galaxies with high ratios of present



to past star formation. The comparison in Fig. 9 suggests that Kennicutt & Kent’s sample contains early-type spirals with preferentially low massive star formation rates. This has also been noted by Usui *et al.* who have obtained  $H\alpha$  fluxes of galaxies with high  $L(\text{fir})/L(\text{blue})$  luminosity ratios and their results are also shown in Figure 9. The images presented in this paper reveal early-type spirals to encompass a wide range of  $H\alpha$  equivalent widths spanning that measured by both Kennicutt & Kent and Usui *et al.*

In an attempt to reconcile the differences in  $H\alpha$  equivalent widths between this study and Kennicutt & Kent (1983), we have examined the morphological classifications of the galaxies. We have noted that Kennicutt & Kent used classifications from the Revised Shapley-Ames Catalog (RSA) (Sandage & Tammann 1981). On the other hand classifications in the NBG catalog (Tully 1988), which are used for this paper, are derived mostly from the Second Reference Catalog (RC2) (de Vaucouleurs *et al.* 1976). Table 5 lists the morphology of the galaxies included in the present study as they appear in the Tully catalog (Tully 1988), the Second Reference Catalog (RC2) (de Vaucouleurs 1976), and the Revised Shapley-Ames Catalog (Sandage & Tammann 1981). Part of the difference in the  $H\alpha$  equivalent widths measured for early-type spirals by us and Kennicutt & Kent can be traced to a difference in galaxy classification. Almost all of the category 2 Sa-Sab galaxies have been classified as Sb’s in the RSA catalog and would have been regarded as such in the study of Kennicutt & Kent.

The systematic difference between RC2 and RSA classifications is surprising and may be traced to subtle variations in the application of the criteria used for classifying spiral galaxies. The classification criteria for the RC2 are explained in *Handbuch der Physik* (de Vaucouleurs 1959), whereas RSA classifications are elaborated in *the Hubble Atlas of Galaxies* (Sandage 1961). In the RC2 catalog, sub-types of spirals, Sa-Sc, are defined by the “*relative importance of the nucleus (decreasing from a to c) and the degree of unwinding and resolution of the arms (increasing from a to c)*” (de Vaucouleurs 1959). Spiral galaxies in RSA catalog are classified according to the same criteria: “*the openness of the spiral arms, the degree of resolution of the arms into stars, and the relative size of the unresolved nuclear region*” (Sandage 1961). However, the third criterion (bulge size) was not considered important for actual classifications in RSA; “*For many years it was thought that the third classification criterion of the relative size of the unresolved nuclear region usually agreed with the criterion of the arms. Inspection of large numbers of photographs shows that, although there is a general correlation of the criteria, there are Sa galaxies that have small nuclear regions. The assignment of galaxies to the Sa, Sb, or Sc type is based here primarily on the characteristics of the arms*” (Sandage 1961). The preceding sentence may provide an explanation for the classification difference found for category 2 galaxies in the RC2 and RSA catalogs. The differences can be quite extreme, for example, NGC 7552 is considered

a prototypical SBab galaxy by de Vaucouleurs (1959) but an SBbc by Sandage in the RSA catalog (Sandage & Tammann 1981).

Over the years, many studies have been conducted analyzing star forming properties of spiral galaxies along the Hubble sequence. Kennicutt & Kent (1983), de Jong (1984), Sandage (1986), Rieke & Lebofsky (1986), Pompea & Rieke (1989), & Caldwell *et al.* (1991) used morphological classifications from RSA catalog and found a dependence of star formation on Hubble types Sa-Scd. However, this is not totally surprising since RSA classifications are primarily based on the arm characteristics, which are tightly correlated with star formation. On the other hand, Devereux and Young (1990), Isobe & Fiegelson (1992), Tomita *et al.* (1996), Young *et al.* (1996), Devereux and Hameed (1997), and Usui *et al.* (1998) have used RC2 classifications and find that star formation rates in spiral (Sa-Scd) galaxies are independent of Hubble type. Similar results were obtained by Gavazzi (1986) and Bothun *et al.* (1989), who used classifications given in the UGC catalog. Thus it appears that perceptions concerning star formation rates among spiral galaxies along the Hubble sequence depends on the choice of catalog. Furthermore, it may be that other Hubble-type correlations also depend on the choice of catalog.

We do not want to claim that the classifications of one catalog are better than the other. However, we do want to stress the importance of the NBG catalog in the study of nearby galaxies. As described earlier, the NBG catalog is the most complete compilation of nearby galaxies. It contains all known galaxies within 40 Mpc that are brighter than 12th magnitude. Any systematic study aimed at understanding the properties of nearby galaxies will rely on the NBG catalog.

Results presented in this paper have exposed the subjective nature of the prevailing classification schemes. Perhaps it is time to start classifying galaxies quantitatively using measures of their physical properties.

## 6. Summary & Conclusions

Preliminary results of an on-going H $\alpha$  imaging survey of nearby, bright, early-type (Sa-Sab) spirals have revealed them to be a heterogeneous class of galaxies. Furthermore, our images have identified a significant number of early-type spirals with massive star formation rates comparable to the most prolifically star forming Sc galaxies. An analysis of the H $\alpha$  images suggests that early-type spirals can be divided into two categories based on the H $\alpha$  luminosity of the largest H II region in the disk. The first category includes galaxies for which the individual H II regions have H $\alpha$  luminosity,  $L_{H\alpha} < 10^{39} \text{ ergs}^{-1}$ . Previously it

was thought that all H II regions in early-type spirals have  $L_{H\alpha} < 10^{39} \text{ergs}^{-1}$ , but our new observations have revealed a second category which includes 15 – 20% of early-type spirals.

Most of the category 1 galaxies appear morphologically undisturbed. Despite the similarities in the continuum images, category 1 galaxies exhibit diverse nuclear properties. The early-type spirals with the lowest H $\alpha$  luminosities host extended nuclear emission line regions whereas the galaxies that have the highest H $\alpha$  luminosities contain nuclear starbursts. We also derived H II region luminosity functions for one galaxy from each category. Our results suggest that, overall, H II regions in category 1 early-type spirals are less luminous than H II regions in category 2 early type spirals and that the difference between the two categories is not due to the existence of a single “anomalous” H II region with  $L_{H\alpha} \geq 10^{39} \text{ergs}^{-1}$ . Dust lanes and tidal tails are present in the continuum images of all category 2 galaxies suggesting a recent interaction, which may also explain the presence of giant H II regions in these galaxies.

The heterogeneous nature of early-type spirals, as revealed by the continuum and H $\alpha$  images, illustrates the problems associated with classifying galaxies morphologically. The results presented in this paper constitute part of an on-going H $\alpha$  survey to image a complete sample of nearby, bright, early-type spirals. It is anticipated that the survey will be the first to quantify the diverse nature of early-type spirals by providing a statistically significant set of observations.

The authors would like to thank Rene’ Walterbos for providing the H $\alpha$  filter set for the APO observations. Thanks also to the TACs at NOAO and APO for the generous allocation of observing time and their staffs for expert assistance at the telescopes. N.D. gratefully acknowledges the National Geographic Society for travel support to CTIO. S.H. would like to thank NOAO for travel support to CTIO, Jon Holtzman, Charles Hoopes, and Bruce Greenawalt for useful comments on the paper, and David Thilker for providing the H II region LF program, ‘HIIphot’. We would also like to thank the referee, Marcella Carollo, for useful comments that improved the presentation of the paper. HIIphot was created by David Thilker under support from NASA’s Graduate Student Researcher Program (NGT-51640). The IDL source code and explanatory documentation will soon be available by request. Contact dthilker@nmsu.edu for details.

## REFERENCES

- Arsenault,R. 1989, A&A, 217, 66  
Ashby,M.L.N., Houck,J.R., & Matthews,K. 1995, ApJ, 447, 545

- Balcells,M., & Peletier,R. 1994, AJ, 107, 135
- Balzano,V.A. 1983, ApJ, 268, 602
- Beitenholz,M.F., et al. 1996, ApJ, 457, 604
- Binette,L., Magris,C.G., Stasinska,G., & Bruzual,A.G. 1994, A&A, 292, 13
- Bothun,G.D., Lonsdale,C.J., & Rice,W. 1989, ApJ, 341, 129
- Braun,R., Walterbos,R.A.M., & Kennicutt,R.C.,Jr. 1992, Nature, 360, 442
- Bresolin,F., & Kennicutt,R.C.,Jr. 1997, AJ113, 975
- Bushouse,H.A. 1987, ApJ, 320, 49
- Caldwell,N, Kennicutt,R.C.,Jr, Phillips,A.C., & Schommer,R.A. 1991, ApJ, 370, 526
- Carollo,C.M., Siavelli,M, & Mack,J. 1998, AJ, 116, 68
- Casoli,F., Sauty,S., Gerin,M., Boselli,A., Fouque,P., Braine,J., Gavazzi,G., Lequeux,J., & Dickey,J. 1998, A&A, 331, 451
- Crocker,D.A., Baugus,P.D., & Buta,R. 1996, ApJS, 105, 353
- Devereux,N.A. 1987, ApJ, 323, 91
- Devereux,N.A., Ford,H., & Jacoby,G. 1997, ApJ, 481, L71
- Devereux,N.A., & Hameed,S. 1997, AJ, 113, 599
- Devereux,N.A., Jacoby,G., & Ciardullo,R. 1995, AJ, 110, 1115
- Devereux,N.A., Price,R., Wells,L.A., & Duric,N. 1994, AJ, 108, 1667
- Devereux,N.A., & Young,J.S. 1990, ApJ, 350, L25
- Eggen,O., Lynden-Bell,D., & Sandage,A., 1962, ApJ, 136, 748
- Elmegreen,B.G., & Elmegreen,D.M. 1985, ApJ, 288, 438
- Fabbiano,G., 1988, ApJ, 325, 544
- Feinstein,C., 1997, ApJS, 112, 29
- Filippenko,A.V., & Halpern,J.P. 1984, ApJ, 285,458
- Filippenko,A.V., & Sargent,W.L.W. 1988, ApJ, 324, 134
- Gavazzi,G., Cocito,A., & Vettolani,G. 1986, ApJ, 305, L15
- Hamuy,M., Suntzeff,N.B., Heathcote,S.R., Walker,A.R., Gigoux,P., & Phillips,M.M. PASP, 106, 566
- Hawarden,T.G., Mountain,C.M., Leggett,S.K., & Puxley,P.J. 1986, MNRAS, 221, 41

- Heckman, T.M. 1996, in *The Physics of LINERS in view of Recent Observations*, ed. Eracleous, M., Koratkar, A., Leitherer, C., & Ho, L. (ASP Conference Series Volume 103)
- Ho, L.C., Filippenko, A.V., & Sargent, W.L.W. 1996, *ApJ*, 462, 183
- Ho, L.C., Filippenko, A.V., & Sargent, W.L.W. 1997, *ApJ*, 487, 568
- Ho, L.C., Filippenko, A.V., & Sargent, W.L.W. 1997a, *ApJS*, 112, 315
- Ho, L.C., Filippenko, A.V., & Sargent, W.L.W. 1997b, *ApJ*, 487, 591
- Hodge, P., & Kennicutt, R.C., Jr. 1983, *AJ*, 88, 296
- Huang, J.H., Gu, Q.S., Su, H.J., Hawarden, T.G., Liao, X.H., & Wu, G.X. 1996, *A&A*, 313, 13
- Hubble, E. 1936, *The Realm of the Nebulae* (New Haven: Yale Univ. Press)
- Isobe, T., & Feigelson, E.D. 1992, *ApJS*, 79, 197
- Jacoby, G.H., Ciardullo, R., Ford, H.C., & Booth, J. 1989, *ApJ*, 344, 704
- Jacoby, G.H., Ford, H.C., & Ciardullo, R. 1985, *ApJ*, 290, 136
- de Jong, T. *et al.* 1984, *ApJ*, 278, 67L
- Keel, W.B. 1983a, *ApJ*, 268, 632
- Keel, W.B. 1983b, *ApJS*, 52, 229
- Kennicutt, R.C., Jr. 1983, *ApJ*, 272, 54
- Kennicutt, R.C., Jr. 1988, *ApJ*, 334, 144
- Kennicutt, R.C., Jr. 1998, *Ann. Rev. Astron. Astrophys.* in press.
- Kennicutt, R.C., Jr., Edgar, K.B., & Hodge, P.W., 1989, 337, 761
- Kennicutt, R.C., Jr., Keel, W.C., van der Hulst, J.M., Hummel, E., & Roettiger, K.A. 1987, *AJ*, 93, 1011
- Kennicutt, R.C., Jr., & Kent, S.M. 1983, *AJ*, 88, 1094
- Kennicutt, R.C., Jr., Tamblyn, P., & Congdon, C.W. 1994, *ApJ*, 435, 22
- King, I.R., et al. 1992, *ApJ*, 397, L35
- Kormendy, J. 1977, in *The Evolution of Galaxies and Stellar Populations*, ed. B.M. Tinsley & R.B. Larson (New Haven: Yale Univ. Obs.), 131
- Larson, R.B., & Tinsley, B.M. 1974, *ApJ*, 192, 293
- Lehnert, M.D., & Heckman, T.M. 1995, *ApJS*, 97, 89
- Liu, C.T., & Kennicutt, R.C., Jr. 1995, *ApJ*, 450, 547

- Maoz,D., et al. 1995, ApJ, 440, 91
- Massey,P., Strobel,K., Barnes,J.V., & Anderson,E. 1988, ApJ, 328, 315
- Merrifield,M.R., & Kuijken,K. 1994, ApJ, 432, 575
- Mihos,J.C., & Hernquist,L. 1994, ApJ, 425, L13
- Peimbert,M., & Torres-Peimbert,S. 1981, ApJ, 245, 845
- Petre,R., Mushotzky,R., Serlemitsos,P.J., Jahoda,K., & Marshall,F.E. 1993, ApJ, 418, 644
- Pfenniger, D. 1991, in *Dynamics of Disc Galaxies*, ed. B. Sundelius, Goteborgs, p. 191
- Pfenniger, D. 1993, in IAU Symp. 153, *Galactic Bulges*, eds. H. Dejonghe and H.T. Habing (Dordrecht, Kluwer), p. 387
- Phillips,M.M., Charles,P.A., & Baldwin,J.A. 1983, ApJ, 266, 485
- Pompea,S.M., & Rieke,G.H. 1989, ApJ, 342, 250
- Puxley,P.J., Hawarden,T.G., & Mountain,C.M. 1988, MNRAS, 231, 465
- Rich,M.R., & Terndrup,D.M. 1997, PASP, 109, 571
- Rieke,G.H., & Lebofsky,M.J. 1986, ApJ, 304, 326
- Rieke,G.H., Lebofsky,M.J., Thompson,R.I., Low,F.J., & Tokunaga,A.T. 1980, ApJ, 238, 24
- Roberts,M.S. 1969, AJ, 74, 859
- Roberts,M.S., & Haynes,M.P. 1994, *Ann. Rev. Astron. Astrophys.*, 32, 115
- Rubin,V.C., & Ford,H. 1971, ApJ, 170, 25
- Ryder,S.D., & Dopita,M.A. 1994, ApJ, 430, 142
- Sandage,A.R. 1961, *The Hubble Atlas of Galaxies*, Publ. No. 618 (Carnegie Institution of Washington, Washington,D.C.)
- Sandage,A.R., A&A, 161, 89
- Sandage,A., & Tammann,G.A. 1981, *A Revised Shapley-Ames Catalog of Bright Galaxies*, Publ. No. 635(Carnegie Institution of Washington, Washington,D.C.) (RSA)
- Schweizer,F., 1978, ApJ, 220, 98
- Schweizer,F. 1990, in *Dynamics and Interactions of Galaxies*, ed. Wielen.R. (Heidelberg: Springer-Verlag)
- Schweizer,F., & Seitzer,P. 1988, ApJ, 328,88
- Sharples,R.M., Longmore,A.J., Hawarden,T.G., and Carter,D. 1984, MNRAS, 208, 15
- Thilker,D., Braun,R., Walterbos,R.A.M., & Fierro,V. 1999, *in prep.*

- Tomita, A., Tomita, Y., and Saito, M. 1996, PASJ, 48, 285
- Tully,R.B. 1988, *Nearby Galaxies Catalog* (Cambridge: Cambridge University Press)
- Unger,S.W., Lawrence,A., Wilson,A.S., Elvis,M., and Wright,A.E. 1987, MNRAS, 228, 521
- Usui, T., Saito, M., and Tomita, A. 1998, AJ, 116, 2166
- de Vaucouleurs, G. 1959, *Handbuch der Physik*, vol. 53, 275 (Berlin: Springer-Verlag)
- de Vaucouleurs, G., de Vaucouleurs,A., & Corwin,H.G. 1976, *Second Reference Catalog of Bright Galaxies* (University of Texas, Austin) (RC2)
- van den Bergh,S. 1976, AJ, 81, 797
- Veron-Cetty,M.P., & Veron,P. 1986, A&AS, 66,335
- Wyse,R.F.G., Gilmore,G., & Franx,M. 1997, *Ann. Rev. Astron. Astrophys.*, 35, 637
- Young,J.S., Allen,L., Kenney,J.D.P., Lesser,A., & Rowand,B. 1996, AJ, 112, 1903
- Young,J.S., Kleinmann,S.G., & Allen.L.E. 1988, ApJ, 334, L63
- Young,J.S., & Knezek,P.M. 1989, ApJ, 347, L55
- Zaritsky, D. 1995, ApJ, 448, L17

Fig. 1.— Comparison of H $\alpha$  flux measurements taken from the literature with those measured from our H $\alpha$  images using the same aperture size. NGC 1022 has two published values for its H $\alpha$  flux (see text for details).

Fig. 2.— Histograms illustrating the distribution of total H $\alpha$  luminosity of Category 1 and Category 2 early-type spirals.

Fig. 3.— Histograms illustrating the distribution of H $\alpha$  equivalent widths of Category 1 and Category 2 early-type spirals.

Fig. 4.— Histograms illustrating the distribution of the nuclear(1kpc) H $\alpha$  luminosity of Category 1 and Category 2 early-type spirals.

Fig. 5.— Red continuum and continuum-subtracted H $\alpha$  images of 17 category 1 early-type spiral galaxies. The white bar at lower left in each image represent 1 kpc in length. North is at the top and east is at the left in each image.

Fig. 6.— Red continuum and continuum-subtracted H $\alpha$  images of 10 category 2 early-type spiral galaxies. The white bar at lower left in each image represent 1 kpc in length. North is at the top and east is at the left in each image.

Fig. 7.— Red continuum and continuum-subtracted H $\alpha$  images of 2 'unclassified' early-type spiral galaxies. The white bar at lower left in each image represent 1 kpc in length. North is at the top and east is at the left in each image.

Fig. 8.— The H II region luminosity function of a Category 1 early-type spiral, NGC 1398, and a Category 2 early-type spiral, NGC 7552.

Fig. 9.— A comparison of H $\alpha$  equivalent widths of all early-type spirals presented in this paper with the H $\alpha$  equivalent widths of Kennicutt & Kent (1983) and Usui *et al.* (1998).



Table 1. Galaxy Parameters<sup>a</sup>

| Galaxy   | m(B)<br>(mag) | size<br>(arc min) | $i$ | $V_h$<br>( $kms^{-1}$ ) | Distance<br>(Mpc) |
|----------|---------------|-------------------|-----|-------------------------|-------------------|
| NGC 660  | 11.37         | 7.2               | 77° | 856                     | 11.8              |
| NGC 972  | 11.75         | 3.9               | 65° | 1539                    | 21.4              |
| NGC 986  | 11.66         | 3.3               | 42° | 1983                    | 23.2              |
| NGC 1022 | 12.13         | 2.5               | 28° | 1503                    | 18.5              |
| NGC 1350 | 11.16         | 5.0               | 62° | 1786                    | 16.9              |
| NGC 1371 | 11.43         | 6.8               | 53° | 1472                    | 17.1              |
| NGC 1398 | 10.47         | 7.6               | 50° | 1401                    | 16.1              |
| NGC 1433 | 10.64         | 5.9               | 27° | 1071                    | 11.6              |
| NGC 1482 | 13.50         | 2.1               | 58° | 1655                    | 19.6              |
| NGC 1515 | 11.17         | 5.7               | 89° | 1169                    | 13.4              |
| NGC 1617 | 10.92         | 4.0               | 65° | 1040                    | 13.4              |
| NGC 2146 | 11.00         | 5.3               | 36° | 918                     | 17.2              |
| NGC 2273 | 11.63         | 3.4               | 50° | 1844                    | 28.4              |
| NGC 3169 | 11.24         | 5.0               | 59° | 1229                    | 19.7              |
| NGC 3471 | 12.98         | 1.9               | 64° | 2076                    | 33.0              |
| 1108-48  | 13.64         | 2.4               | 53° | 2717                    | 35.2              |
| NGC 3717 | 11.87         | 6.1               | 90° | 1731                    | 24.6              |
| NGC 3885 | 12.56         | 2.9               | 77° | 1948                    | 27.8              |
| NGC 5156 | 11.92         | 2.4               | 24° | 2983                    | 39.5              |
| NGC 5188 | 12.58         | 3.8               | 74° | 2366                    | 32.9              |
| NGC 5728 | 11.75         | 2.3               | 65° | 2970                    | 42.2              |
| NGC 5915 | 11.88         | 1.4               | 42° | 2272                    | 33.7              |
| NGC 6810 | 11.40         | 3.2               | 82° | 1995                    | 25.3              |
| NGC 7172 | 12.55         | 2.1               | 64° | 2651                    | 33.9              |
| NGC 7213 | 11.35         | 2.1               | -   | 1778                    | 22.0              |
| NGC 7552 | 11.31         | 3.5               | 31° | 1609                    | 19.5              |
| NGC 7582 | 11.06         | 4.5               | 65° | 1459                    | 17.6              |

<sup>a</sup>From Tully (1988)

Table 2. Details of Observations

| Galaxy   | Epoch       | Telescope | H $\alpha$ filter | Exp. time | Standard   | Ref. |
|----------|-------------|-----------|-------------------|-----------|------------|------|
| NGC 660  | 1996 Aug 14 | APO 3.5m  | 6570/72           | 600s      | BD+28°4211 | 1    |
| NGC 972  | 1996 Aug 14 | APO 3.5m  | 6610/70           | 600s      | BD+28°4211 | 1    |
| NGC 986  | 1997 Oct 23 | CTIO 1.5m | 6606/75           | 900s      | LTT 1020   | 2    |
| NGC 1022 | 1997 Oct 25 | CTIO 1.5m | 6606/75           | 900s      | LTT 7987   | 2    |
| NGC 1350 | 1997 Oct 24 | CTIO 1.5m | 6606/75           | 900s      | LTT 7987   | 2    |
| NGC 1371 | 1997 Oct 25 | CTIO 1.5m | 6606/75           | 900s      | LTT 7987   | 2    |
| NGC 1398 | 1997 Oct 24 | CTIO 1.5m | 6606/75           | 900s      | LTT 7987   | 2    |
| NGC 1433 | 1997 Oct 26 | CTIO 1.5m | 6606/75           | 900s      | LTT 7987   | 2    |
| NGC 1482 | 1996 Nov 10 | APO 3.5m  | 6610/70           | 720s      | G191B2B    | 1    |
| NGC 1515 | 1997 Oct 26 | CTIO 1.5m | 6606/75           | 900s      | LTT 7987   | 2    |
| NGC 1617 | 1997 Oct 23 | CTIO 1.5m | 6606/75           | 900s      | LTT 1020   | 2    |
| NGC 2146 | 1996 Nov 10 | APO 3.5m  | 6570/72           | 720s      | G191B2B    | 1    |
| NGC 2273 | 1997 Jan 30 | APO 3.5m  | 6610/70           | 550s      | G191B2B    | 1    |
| NGC 3169 | 1997 Mar 16 | CTIO 1.5m | 6606/75           | 900s      | LTT 3218   | 2    |
| NGC 3471 | 1997 Jan 30 | APO 3.5m  | 6610/70           | 550s      | G191B2B    | 1    |
| 1108-48  | 1997 Mar 15 | CTIO 1.5m | 6606/75           | 900s      | LTT 3218   | 2    |
| NGC 3717 | 1997 Mar 15 | CTIO 1.5m | 6606/75           | 900s      | LTT 3218   | 2    |
| NGC 3885 | 1997 Mar 16 | CTIO 1.5m | 6606/75           | 900s      | LTT 3218   | 2    |
| NGC 5156 | 1997 Mar 16 | CTIO 1.5m | 6606/75           | 900s      | LTT 3218   | 2    |
| NGC 5188 | 1997 Mar 15 | CTIO 1.5m | 6606/75           | 900s      | LTT 3218   | 2    |
| NGC 5728 | 1997 Mar 15 | CTIO 1.5m | 6649/76           | 900s      | LTT 3218   | 2    |
| NGC 5915 | 1997 Mar 16 | CTIO 1.5m | 6606/75           | 900s      | LTT 3218   | 2    |
| NGC 6810 | 1997 Oct 24 | CTIO 1.5m | 6606/75           | 900s      | LTT 7987   | 2    |
| NGC 7172 | 1997 Oct 26 | CTIO 1.5m | 6606/75           | 900s      | LTT 7987   | 2    |
| NGC 7213 | 1997 Oct 25 | CTIO 1.5m | 6606/75           | 900s      | LTT 7987   | 2    |
| NGC 7552 | 1997 Oct 24 | CTIO 1.5m | 6606/75           | 900s      | LTT 7987   | 2    |
| NGC 7582 | 1997 Oct 23 | CTIO 1.5m | 6606/75           | 900s      | LTT 7987   | 2    |

References. — (1) Massey et al. 1988; (2) Hamuy et al. 1994.

Table 3. Summary of Results

| Galaxy                        | $F_{[H\alpha+N[II]]}^a$<br>( $10^{-12} \text{ ergs}^{-1} \text{ cm}^{-2}$ ) | Aperture<br>(arcsec) | $L_{H\alpha}$<br>( $10^{40} \text{ ergs}^{-1}$ ) | $L_{H\alpha}(1kpc)$<br>( $10^{40} \text{ ergs}^{-1}$ ) | $L_{H\alpha}(1kpc)/L_{H\alpha}$ |
|-------------------------------|---|----------------------|--|--|---------------------------------|
| Category 1 Early-type Spirals |   |                      |  |  |                                 |
| NGC 7213                      | 2.9±0.4   | 210.7                | 16.8   | 5.2  | 31%                             |
| NGC 3169                      | 3.0±0.5   | 217.2                | 13.9   | 0.7  | 5%                              |
| NGC 5728                      | 0.6±0.2   | 75.3                 | 12.6   | 0.9  | 7%                              |
| NGC 3717                      | 1.6±0.2   | 180.6                | 11.6   | 1.5  | 13%                             |
| NGC 5188                      | 0.9±0.1   | 77.4                 | 11.0   | 3.0  | 27%                             |
| NGC 1398                      | 3.3±1.2   | 215.0                | 10.3   | 0.3  | 3%                              |
| NGC 3471                      | 0.7±0.1   | 20.4                 | 8.9  | 5.1  | 57%                             |
| NGC 3885                      | 0.9±0.1   | 51.6                 | 8.5  | 5.7  | 67%                             |
| NGC 1482                      | 1.6±0.2   | 48.9                 | 7.4  | 3.7  | 50%                             |
| NGC 1022                      | 1.2±0.2   | 77.4                 | 4.9  | 4.0  | 82%                             |
| NGC 1371                      | 1.4±0.5   | 193.5                | 4.9  | 0.3  | 6%                              |
| NGC 1350                      | 1.3±0.7   | 176.3                | 4.5  | 0.2  | 4%                              |
| NGC 1433                      | 2.3±0.8   | 197.8                | 3.7  | 0.7  | 19%                             |
| NGC 7172                      | 0.3±0.1   | 53.8                 | 3.6  | 0.7  | 19%                             |
| NGC 2273                      | 0.7±0.2   | 103.7                | 2.3  | 1.6  | 70%                             |
| NGC 1515                      | 0.9±0.2   | 307 × 172            | 1.8  | 0.4  | 22%                             |
| NGC 1617                      | 0.6±0.6   | 111.8                | 1.4  | 0.2  | 14%                             |
| Category 2 Early-type Spirals |   |                      |  |  |                                 |
| NGC 5915                      | 3.3±0.2   | 43.0                 | 44.9   | 2.7  | 6%                              |
| NGC 5156                      | 2.2±0.1   | 103.2                | 41.2   | 0.3  | 0.7%                            |
| NGC 7552                      | 7.0±0.7   | 116.1                | 31.9   | 16.0   | 50%                             |
| NGC 986                       | 3.3±0.4   | 114.0                | 21.3   | 6.3  | 30%                             |
| NGC 972                       | 3.7±0.2   | 58.6                 | 20.3   | 1.8  | 9%                              |
| NGC 6810                      | 2.6±0.2   | 86.0                 | 20.0   | 6.9  | 35%                             |
| 1108-48                       | 1.2±0.1   | 137.6                | 17.8   | 0.6  | 3%                              |
| NGC 7582                      | 4.6±0.7   | 139.8                | 17.1   | 7.4  | 43%                             |
| Unclassified <sup>b</sup>     |   |                      |  |  |                                 |
| NGC 2146                      | 4.6±1.0   | 119.0                | 16.3   | 2.8  | 17%                             |
| NGC 660                       | 2.2±0.3   | 163 × 253            | 3.7  | 0.6  | 16%                             |

<sup>a</sup>Fluxes have not been corrected for Galactic or internal extinction.

<sup>b</sup>These galaxies exhibit characteristics of both categories. See text for details.

Table 4. Summary of Results II

| Galaxy                        | Nuc. morph. <sup>a</sup> | Nuc. Sp. class | Ref. | Bar | Comments   |
|-------------------------------|--------------------------|----------------|------|-----|--|
| Category 1 Early-type Spirals |                          |                |      |     |  |
| NGC 7213                      | PS/ENER                  | S1             | 1    | N   | A giant H $\alpha$ filament is located approximately 17 kpc south of the galaxy with no counterpart in the continuum image.              |
| NGC 3169                      | ENER                     | L2             | 2    | N   |  |
| NGC 5728                      | PS                       | S2             | 3    | X   | A tightly wound inner spiral arm and a loose outer spiral arm in the continuum   |
| NGC 3717                      | ?                        | H              | 4    | N   | A prominent dust lane parallel to the major axis of the galaxy   |
| NGC 5188                      | PS                       | H              | 4    | Y   |  |
| NGC 1398                      | ENER                     | N              | 5    | Y   | A bar-ring morphology in H $\alpha$ .  |
| NGC 3471                      | SB                       | H              | 6    | ?   |  |
| NGC 3885                      | SB                       | H              | 7    | N   |  |
| NGC 1482                      | SB                       | ...            | ...  | ?   | A prominent dust lane parallel to the major axis of the galaxy. Filaments and/or chimneys of ionized gas extending perpend. to the disk. |
| NGC 1022                      | SB                       | H              | 8    | Y   | A tightly wound inner spiral arm and a loose outer spiral arm in the continuum   |
| NGC 1371                      | ENER                     | ...            | ...  | X   |  |
| NGC 1350                      | ENER                     | N              | 4    | Y   | A bar-ring morphology in H $\alpha$ .  |
| NGC 1433                      | ENER                     | N              | 4    | Y   | A tightly wound inner spiral arm and a loose outer spiral arm in the continuum   |
| NGC 7172                      | PS                       | S2             | 8    | ?   | A bar-ring morphology in H $\alpha$ .  |
| NGC 2273                      | PS                       | S2             | 2    | Y   | A tightly wound inner spiral arm and a loose outer spiral arm in the continuum   |
| NGC 1515                      | ENER                     | ...            | ...  | X   | A prominent dust lane parallel to the major axis of the galaxy   |
| NGC 1617                      | ENER                     | ...            | ...  | ?   |  |
| Category 2 Early-type Spirals |                          |                |      |     |  |
| NGC 5915                      | ...                      | ...            | ...  | Y   | Asymmetric spiral arms in the continuum. H $\alpha$ morphology does not correspond with the major continuum features.                    |
| NGC 5156                      | ...                      | ...            | ...  | Y   |  |
| NGC 7552                      | ...                      | H              | 4    | Y   | A dwarf galaxy at the end of the northern spiral arm   |
| NGC 986                       | ...                      | H              | 4    | Y   | A tidally disrupted dwarf galaxy at the end of the northern arm?   |
| NGC 972                       | ...                      | H              | 2    | ?   | Dusty morphology. A possible bar-like structure crossing the nucleus   |
| NGC 6810                      | ...                      | S2             | 4    | N   | A prominent dust lane parallel to the major axis of the galaxy   |
| 1108-48                       | ...                      | ...            | ...  | Y   | A faint tidal tail leading to a star forming region 18 kpc north-east of the nuc.  |
| NGC 7582                      | ...                      | S2             | 9    | Y   | A prominent dust lane parallel to the major axis of the galaxy   |
| Unclassified <sup>b</sup>     |                          |                |      |     |  |
| NGC 2146                      | ...                      | H              | 2    | Y   | Highly disturbed morphology with a prominent dust lane   |
| NGC 660                       | ...                      | T2/H           | 2    | Y   | Highly disturbed morph. Two prominent dust lanes perpend. to each other  |

<sup>a</sup>Nuclear regions of all category 2 and unclassified galaxies are resolved in H $\alpha$  , but they do not meet the starburst or the ENER criteria as defined in the text. Hence their nuclear regions have not been classified morphologically.

<sup>b</sup>These galaxies exhibit characteristics of both categories. See text for details.

Note. — H $\alpha$  nuclear morphology: PS=Unresolved point source, ENER=Extended Nuclear Emission Line Region, SB=nuclear starburst

Classification of the nuclear spectrum: S=Seyfert, H=HII nucleus, L=LINER, T=Transition, N=Seyfert-like, i.e. H $\alpha$  < 1.2  $\times$  [NII] $\lambda$ 6583

Bar classifications are taken from Tully (1988) : Y=Bar is present, N=Bar is absent, X=intermediate case, ?=No information.

References. — (1)Filippenko & Halpern 1984; (2) Ho, Filippenko, and Sargent 1997; (3) Phillips, Charles, and Baldwin 1983; (4)Veron-Cetty & Veron 1986; (5) Balzano 1983; (6) Lehnert & Heckman 1995; (7) Ashby et al. 1995; (8) Sharples, Longore, and Hawarden 1984; (9) Unger et al. 1987

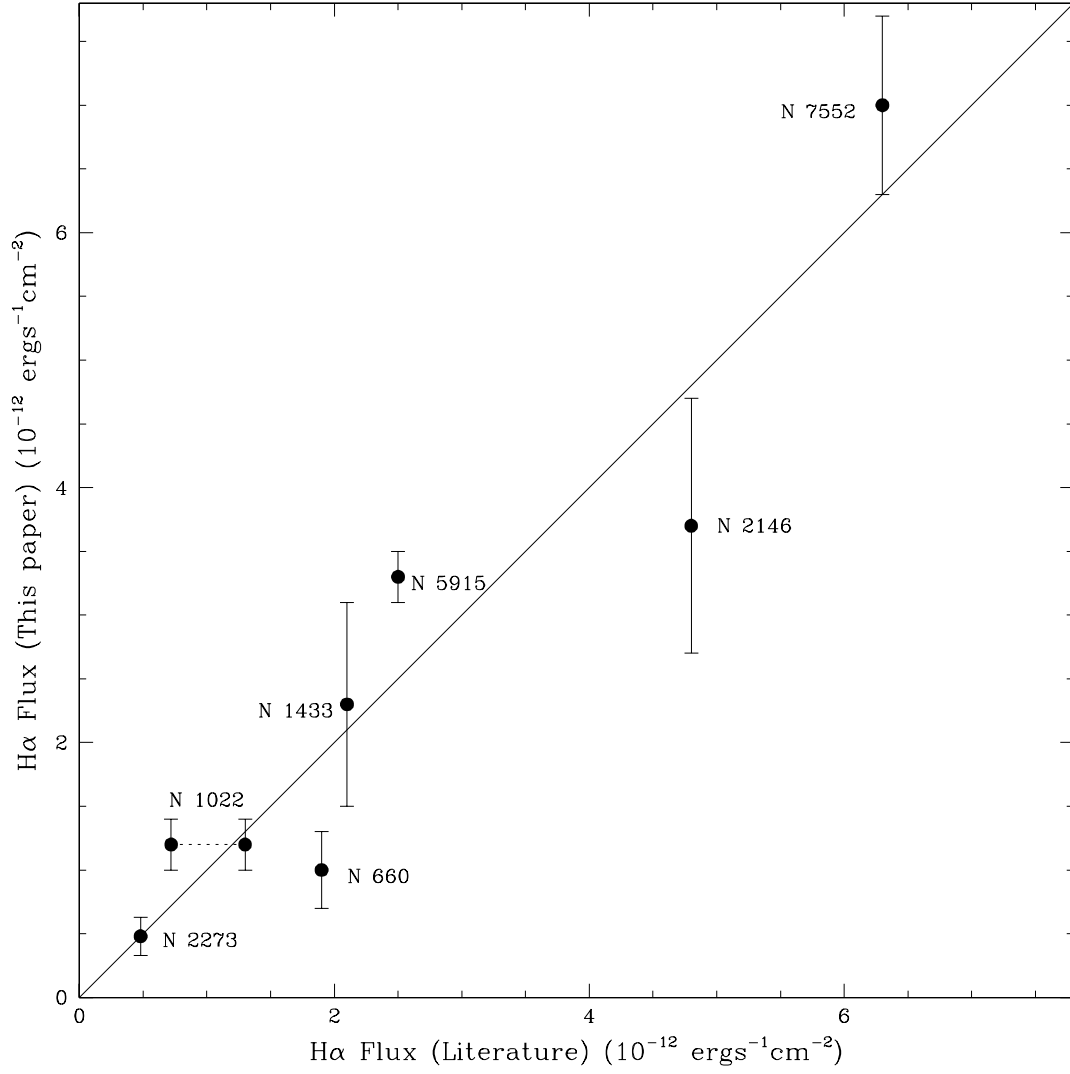
Table 5. Morphological Classifications

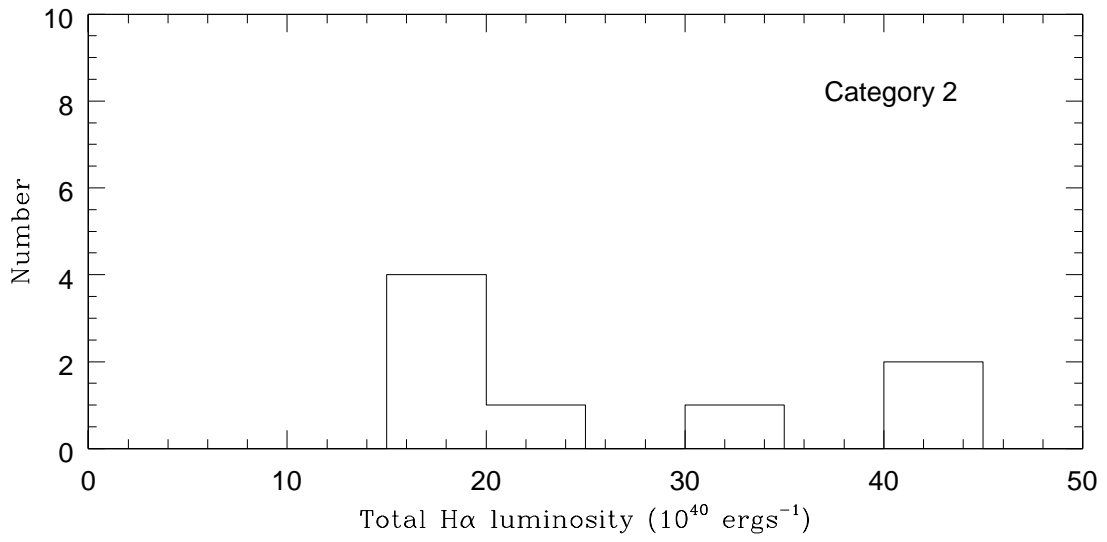
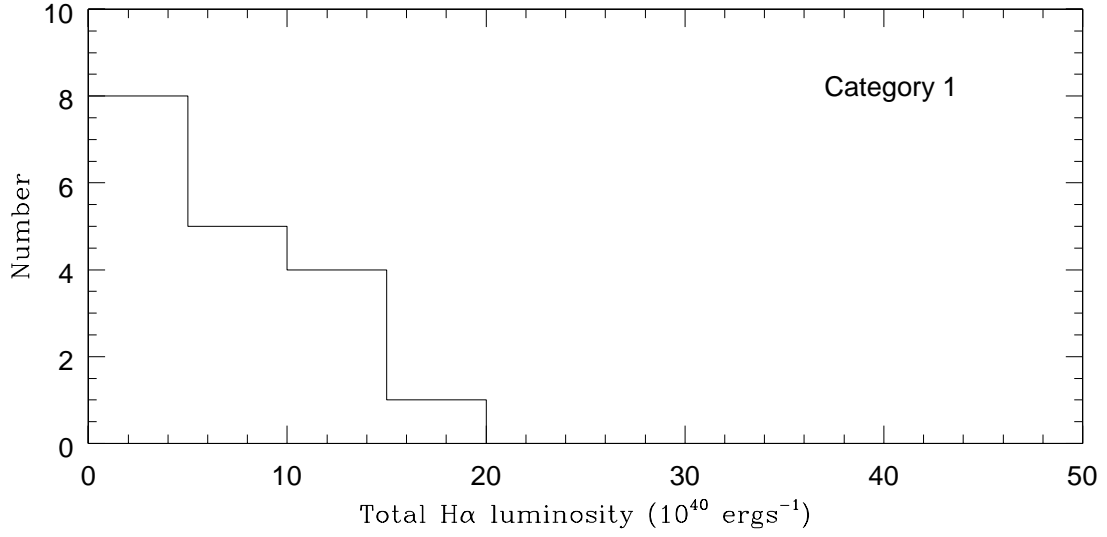
| Galaxy                        | NBG <sup>a</sup> | RC2 <sup>b</sup> | RSA <sup>c</sup> |
|-------------------------------|------------------|------------------|------------------|
| Category 1 Early-type Spirals |                  |                  |                  |
| NGC 7213                      | Sa               | Sa               | Sa               |
| NGC 3169                      | Sa               | Sa               | Sb               |
| NGC 5728                      | Sa               | Sa               | Sb               |
| NGC 3717                      | Sab              | Sb               | Sb               |
| NGC 5188                      | Sa               | Sb               | Sbc              |
| NGC 1398                      | Sab              | Sab              | Sab              |
| NGC 3471                      | Sa               | Sa               | ...              |
| NGC 3885                      | Sa               | S0/a             | Sa               |
| NGC 1482                      | Sa               | S0/a             | ...              |
| NGC 1022                      | Sa               | Sa               | Sa               |
| NGC 1371                      | Sa               | Sa               | Sa               |
| NGC 1350                      | Sab              | Sab              | Sa               |
| NGC 1433                      | Sa               | Sa               | Sb               |
| NGC 7172                      | Sab              | Sab              | ...              |
| NGC 2273                      | Sa               | S0/a             | ...              |
| NGC 1515                      | Sa               | Sbc              | Sb               |
| NGC 1617                      | Sa               | Sa               | Sa               |
| Category 2 Early-type Spirals |                  |                  |                  |
| NGC 5915                      | Sab              | Sab              | Sbc              |
| NGC 5156                      | Sa               | Sab              | Sbc              |
| NGC 7552                      | Sab              | Sab              | Sbc              |
| NGC 986                       | Sab              | Sab              | Sb               |
| NGC 972                       | Sab              | S0/a             | Sb               |
| NGC 6810                      | Sa               | Sab              | Sb               |
| 1108-48                       | Sab              | ...              | ...              |
| NGC 7582                      | Sab              | Sab              | Sab              |
| Unclassified                  |                  |                  |                  |
| NGC 2146                      | Sab              | Sab              | Sb               |
| NGC 660                       | Sa               | Sa               | ...              |

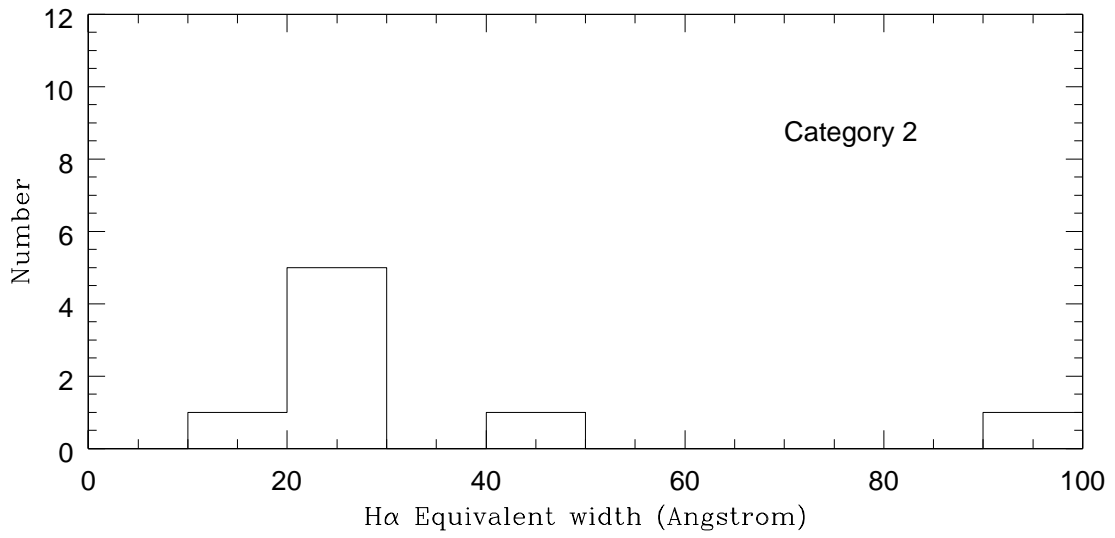
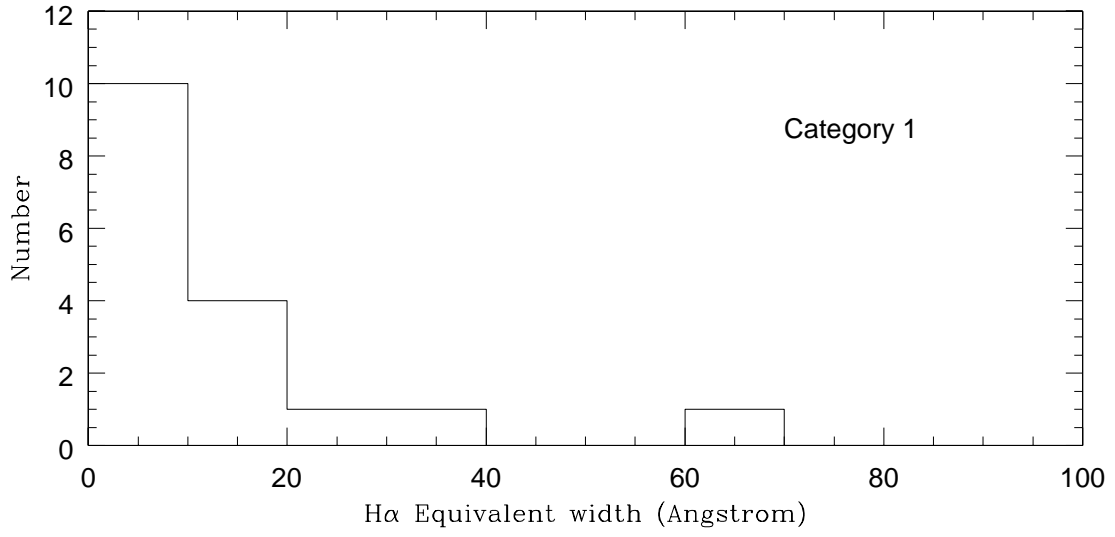
<sup>a</sup> *Nearby Galaxies Catalog*, Tully 1988.

<sup>b</sup> *Second Reference Catalogue of Bright Galaxies*, de Vaucouleurs 1976.

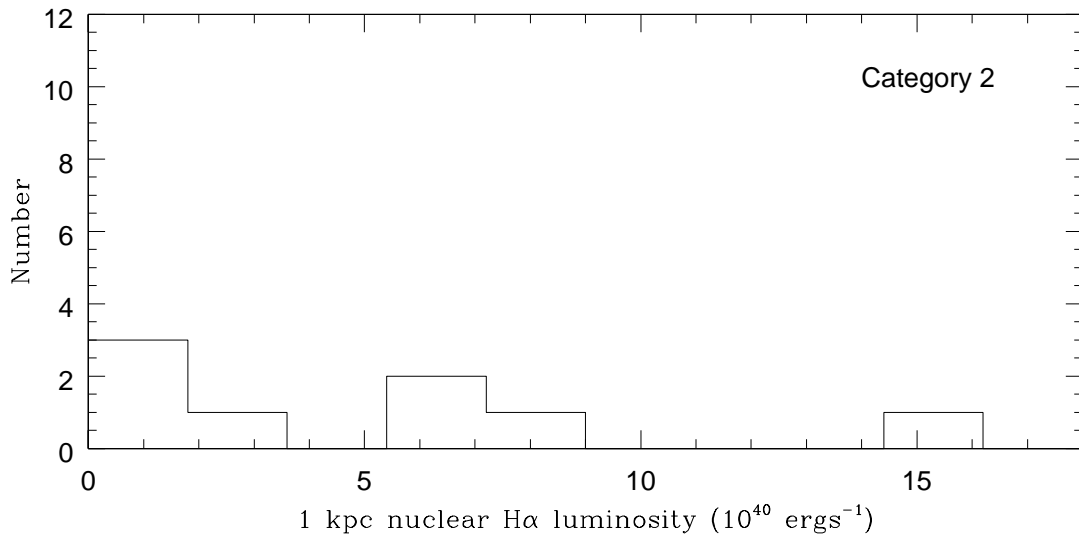
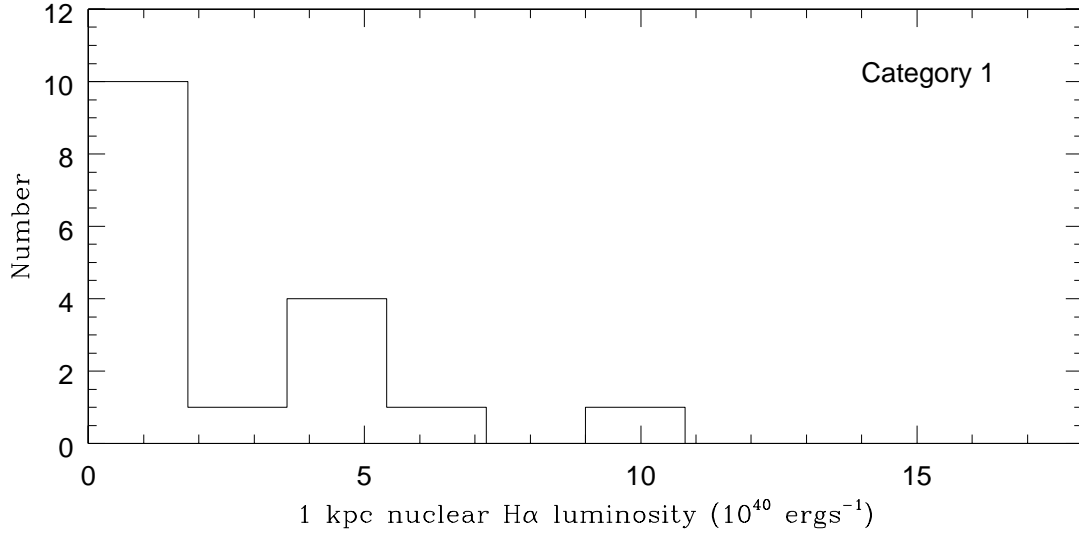
<sup>c</sup> *A Revised Shapley-Ames Catalog of Bright Galaxies*, Sandage & Tammann 1981.

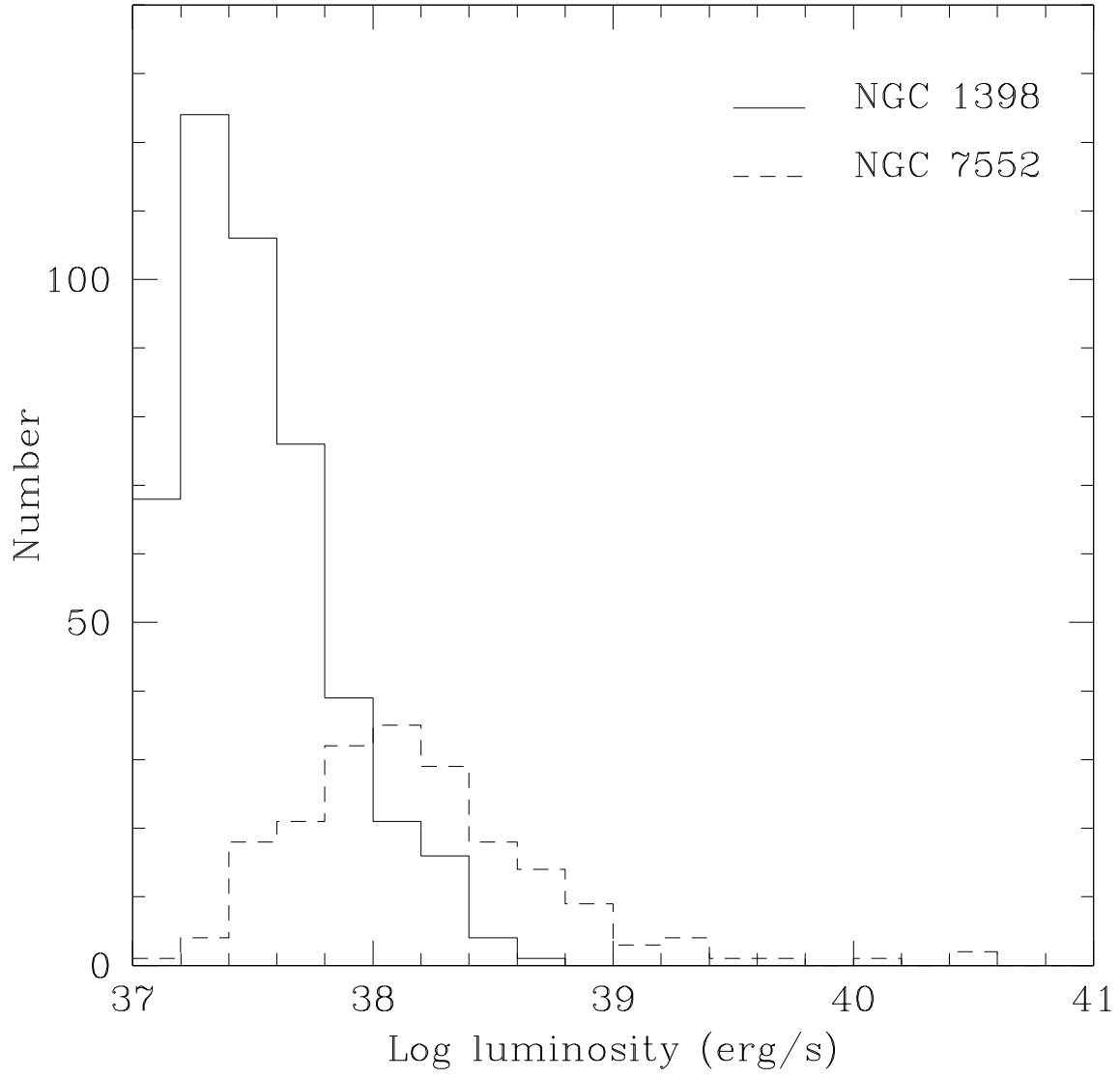


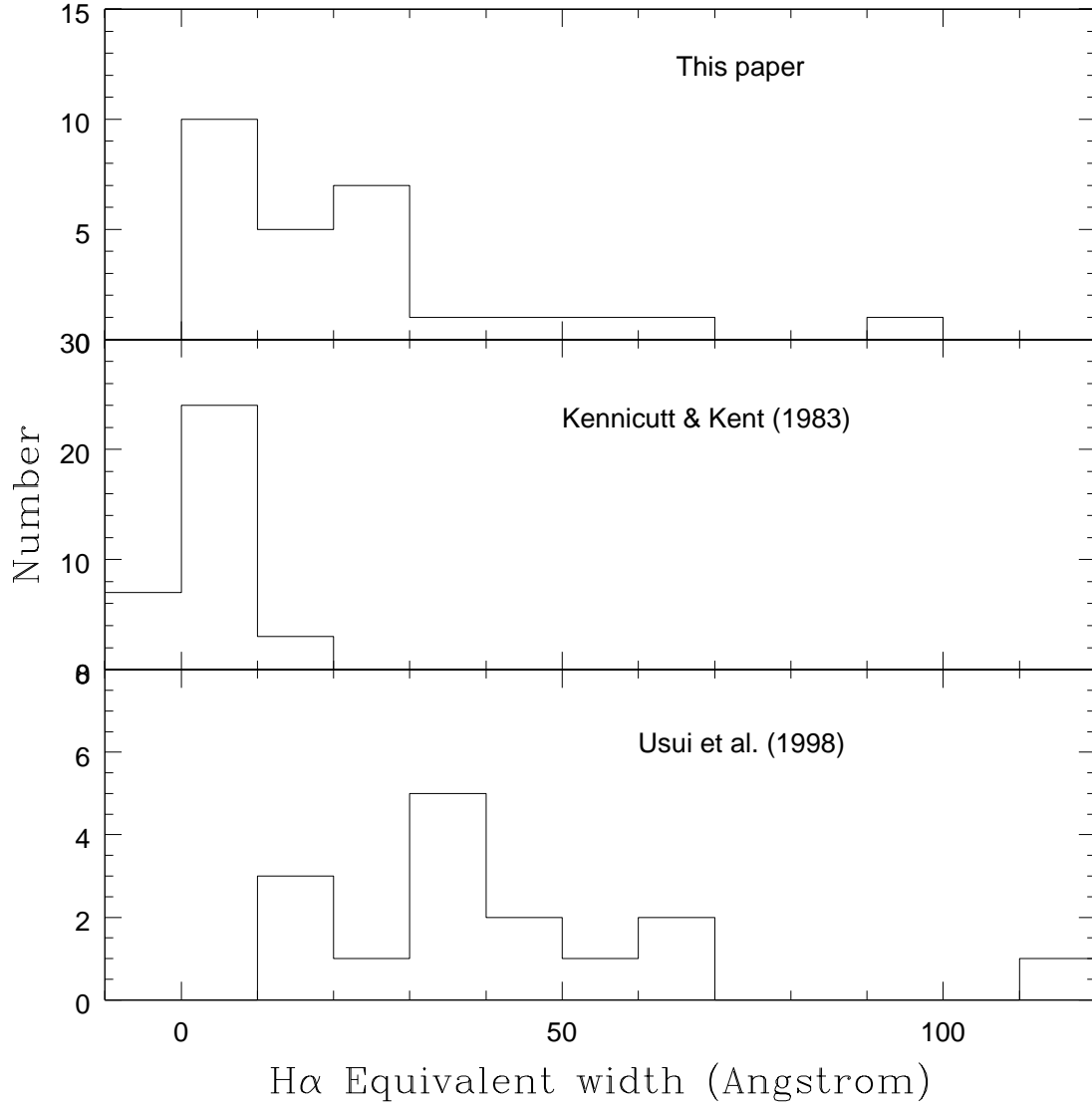












This figure "fig5a.jpg" is available in "jpg" format from:

<http://arxiv.org/ps/astro-ph/9904402v1>

This figure "fig5b.jpg" is available in "jpg" format from:

<http://arxiv.org/ps/astro-ph/9904402v1>

This figure "fig5c.jpg" is available in "jpg" format from:

<http://arxiv.org/ps/astro-ph/9904402v1>

This figure "fig5d.jpg" is available in "jpg" format from:

<http://arxiv.org/ps/astro-ph/9904402v1>

This figure "fig5e.jpg" is available in "jpg" format from:

<http://arxiv.org/ps/astro-ph/9904402v1>



This figure "fig5f.jpg" is available in "jpg" format from:

<http://arxiv.org/ps/astro-ph/9904402v1>

This figure "fig6a.jpg" is available in "jpg" format from:

<http://arxiv.org/ps/astro-ph/9904402v1>

This figure "fig6b.jpg" is available in "jpg" format from:

<http://arxiv.org/ps/astro-ph/9904402v1>

This figure "fig6c.jpg" is available in "jpg" format from:

<http://arxiv.org/ps/astro-ph/9904402v1>

This figure "fig7.jpg" is available in "jpg" format from:

<http://arxiv.org/ps/astro-ph/9904402v1>